Diversity of fungi associated with *Monochamus alternatus* larval habitats in *Bursaphelenchus xylophilus*-infected *Pinus massoniana* and identification of two new ophiostomatalean species (Ascomycota, Ophiostomatales)

Guiheng Zheng[1], Minqi You[2], Xuening Li[3], Qinzheng Zhou[1],
Zheng Wang[1], Huimin Wang[1], Quan Lu[1]

1 *Key Laboratory of Forest Protection, National Forestry and Grassland Administration; Ecology and Nature Conservation Institute, Chinese Academy of Forestry, Beijing 100091, China* **2** *Agriculture and Rural Affairs Bureau of Huangyan District, Taizhou City 318020, China* **3** *Research Institute of Desertification, Chinese Academy of Forestry, Beijing 100091, China*

Corresponding authors: Huimin Wang (whuimin19@126.com), Quan Lu (luquan@caf.ac.cn)

Abstract

Bursaphelenchus xylophilus, a pathogenic pine wood nematode (PWN), is responsible for pine wilt disease (PWD), which has caused significant economic and ecological damage worldwide, particularly in East Asia. Multiple biological factors, such as the beetle vector *Monochamus*, symbiotic bacteria and associated fungi, are involved in the disease infection cycle. This study isolated and identified the fungal communities of *Monochamus alternatus* larval galleries and pupal chambers from different instars through field investigation, morphological observation and multi-locus DNA sequence analyses in Zhejiang Province, China. A total of 255 and 454 fungal strains were isolated from *M. alternatus* galleries and pupal chambers infected with PWN, from the 2nd–3rd and 4th–5th instar larvae, respectively. A total of 18 species of fungi were identified, 14 species were isolated from the 2nd–3rd instar larval galleries and six species from the galleries and pupal chambers of the 4th–5th instar larvae. Amongst them were six species belonging to four genera of ophiostomatalean fungi, including two novel species, *Graphilbum xianjuensis* **sp. nov.** and *Ophiostoma taizhouense* **sp. nov.** and four known species,

Ceratocystiopsis weihaiensis, *Ophiostoma ips*, *Sporothrix zhejiangensis* and *S. macroconidia*. The findings revealed that the fungal diversity and abundance of the 2nd–3rd instar larvae differed markedly from those of the 4th–5th instar larvae. This difference could be the result of fungal succession. This study provides a thorough understanding of the fungi associated with PWD and lays the groundwork for future research.

Introduction

The pine wood nematode (PWN), *Bursaphelenchus xylophilus* (Steiner & Buhrer) Nickle, is a pathogenic nematode that is responsible for the devastating epidemic of pine wilt disease (PWD) worldwide (Mota and Vieira 2008; Robertson et al. 2011), particularly throughout Japan, Korea and China (Togashi and Jikumaru 2007; Jung et al. 2010; Abelleira et al. 2011; Foit et al. 2019). Since the first report in Nanjing, China, in 1982, PWD has spread through more than 700 counties in 19 provinces (State Forestry Administration of the People's Republic of China 2021), killing over one billion pine trees (Zhu et al. 2021). Economic and ecological losses have totalled thousands of billions of Chinese Yuan. PWN has diverse carriers and hosts. Carriers include more than eight beetle species and at least 25 hosts are susceptible under natural conditions (Zheng et al. 2021). In China, the primary PWN vector is the sawyer beetle *Monochamus alternatus* Hope (Coleoptera, Cerambycidae), while *Pinus massoniana* is one of the earliest and most susceptible hosts (Linit et al. 1983; Kobayashi et al. 1984; Ye 2019; Ji et al. 2021).

The PWN is the predominant pathogen in this complex ecosystem (Zhao et al. 2014). The symbiotic interaction between the PWN-vector and fungi is a key biological factor that promotes PWN pathogenicity and invasiveness (Zhao et al. 2014; Zhao and Sun 2017). Molecular analysis has repeatedly demonstrated that the fungus and the PWN have a close symbiotic relationship, as evidenced by the draft genome sequence of a PWN inbred line which revealed that all PWN cellulases were most likely acquired independently from fungi (Kikuchi et al. 2011). Metagenomic analysis of the PWN microbiome indicates that the PWN and its microbiome have established a potentially mutualistic symbiotic relationship with complementary pathways in detoxification metabolism (Kikuchi et al. 2011; Cheng et al. 2013).

Current research has shown that PWN has an important mycetophagous phase in its life history (Ryss et al. 2005; Espada et al. 2016). Many airborne fungi, including endophytes (*Botrytis cinerea* and *Cladosporium herbarum*) and pathogens (*Sirococcus conigenus* and *Sphaeropsis sapinea*), are positively correlated with the growth of the nematode population (Pimentel et al. 2021), with ophiostomatalean fungi (Ascomycota: Sordariomycetes: Ophiostomatales) particularly important in terms of

their association with PWN-*M. alternatus* symbionts. The Ophiostomatales order includes one family (Ophiostomataceae) and twenty genera (*Afroraffaelea*, *Aureovirgo*, *Ceratocystiopsis*, *Chrysosphaeria*, *Dryadomyces*, *Esteya*, *Fragosphaeria*, *Graphilbum*, *Grosmannia*, *Hawksworthiomyces*, *Harringtonia*, *Heinzbutinia*, *Intubia*, *Jamesreidia*, *Leptographium*, *Masuyamyces*, *Ophiostoma*, *Paleoambrosia*, *Raffaelea* and *Sporothrix*) (de Beer et al. 2014, 2016, 2022; Hyde et al. 2020; Wijayawardene et al. 2022). *Sporothrix* sp.1, for example, induces the xylem tissue of the pine tree to produce diacetone alcohol, which may increase PWN propagation and beetle larvae growth (Zhao et al. 2013). PWN produces ascarosides that promote fungal (*Leptographium pini-densiflora* and *Sporothrix* sp.1) growth and sporulation (Zhao et al. 2018). In addition, some fungi are detrimental to PWN. *Esteya vermicola* is an example of direct antagonism (Wang et al. 2011). The lunate conidia of *E. vermicola* are highly infectious to PWN (Liou et al. 1999).

The invasion of beetles altered the internal habitat and mycoflora of pine trees (Zhang et al. 2021). Fungal invasion patterns in beetle-infested hosts may have been successional. *Ips typographus*, for example, attacked Norway spruce with the virulent *Ceratocystis polonica*, followed by other beetle-diffused *Graphium* and *Ophiostoma* fungi (Solheim 1992a, 1992b); *Tomicus minor* invaded *Pinus sylvestris* with *Hormonema dematioides* first, followed by *Ophiostoma tingens* and *O. canum* (Jankowiak 2008). *Ophiostoma ips* was not isolated from the 2nd–3rd instar larvae galleries of *M. alternatus*, but the isolation rate from the 4th–5th instar larvae galleries was 92.5% (Lun et al. 2019). The diversity and abundance of fungi associated with *M. alternatus* larvae of different instars in PWN-infected pines, as well as the successional pattern of fungi in PWN-*M. alteratus* symbionts are unknown. To date, 14 ophiostomatalean fungi have been obtained from *M. alternatus* galleries and pupal chambers along with PWN (Zhao et al. 2013, 2014, 2018; Wang et al. 2018; Lun et al. 2019). However, these studies are sporadic reports and no systematic studies have been conducted.

This research aimed to compare the diversity of fungi in different instars of the PWN-infected *M. alternatus* larval galleries and pupal chambers in south-eastern China. Field surveys were used in conjunction with integrated morphological observation and multi-locus DNA sequence analysis to describe the diversity of fungi associated with PWN and *M. alternatus*. This study provides a scientifically reliable and theoretical foundation for effective PWD control from the fungal perspective.

Materials and methods

Collection of samples and fungal isolations

From October to November 2020, fungi were isolated from 380 and 510 samples of different instars from *M. alternatus* larvae galleries and pupal chambers in *Pinus massoniana*, respectively, in the Huangyan District (28°56'90"N, 121°17'56"E), Xianju County (28°75'28"N, 120°59'97"E), Zhejiang Province. All the trees used

in this study showed signs of death and sap stains and PWNs were simultaneously isolated from galleries and pupal chambers by Behrman funnel. The samples were collected by hand saw, individually placed in sterile envelopes, stored at 4 °C and separated within a week. The surfaces of galleries and pupal chambers were disinfected with 1.5% sodium hypochlorite for 1 min, rinsed with sterile water three times and then cut into approximately 3×3 mm² tissue blocks. They were then inoculated on to a 2% (w/v) water agar medium (20 g agar powder in 1 l of deionised water) and cultured in the dark at 25 °C (Seifert et al. 1993; Wang et al. 2019; Wang et al. 2020). Subsequently, all strains were purified by hyphal tip isolation (Eckhardt 2002) and transferred on to 2% (w/v) malt extract agar (MEA: 20 g malt extract powder and 20 g agar powder in 1 l of deionised water) for growth in the dark at 25 °C. All strains were deposited at the Chinese Academy of Forestry (Table 1). Representative cultures were deposited at the China Forestry Culture Collection Center (CFCC) (Table 2).

Culture and morphological studies

The growth of representative strains was monitored daily and the culture characteristics of the colonies were recorded. Microscopic features were observed using a BX51

Table 1. Species of the fungi isolated from *Pinus massoniana* infected by *Monochamus alternates* and *Bursaphelenchus xylophilus* in the current study.

Taxon	Species	2nd–3rd instar larvae		4th~5th instar larvae	
		number	isolation rate	number	isolation rate
1	*Ceratocystiopsis weihaiensis*	3	1.18%	N/A	N/A
	Chaetomium globosum	1	0.39%	N/A	N/A
	Colletotrichum gloeosporioides	8	3.14%	N/A	N/A
	Cytospora sp.	11	4.31%	N/A	N/A
	Diplodia sapinea	27	10.59%	76	16.74%
	Fusarium sp.	10	3.92%	N/A	N/A
2	*Graphilbum* sp.	N/A	N/A	12	2.64%
3	*Ophiostoma ips*	N/A	N/A	231	50.88%
4	*Ophiostoma* sp.	62	24.31%	N/A	N/A
	Penicillium sp.	2	0.78%	5	1.10%
	Pestalotiopsis sp.	N/A	N/A	2	0.44%
	Phialocephala sp.	45	17.65%	N/A	N/A
	Pseudocosmospora sp.	14	5.49%	N/A	N/A
	Schizophyllum sp.	8	3.14%	N/A	N/A
5	*Sporothrix macroconidia*	4	1.57%	N/A	N/A
6	*S. zhejiangensis*	8	3.14%	N/A	N/A
	Trichoderma atroviride	N/A	N/A	107	23.57%
	Xenoacremonium sp.	37	14.51%	N/A	N/A
	Unidentified	15	5.88%	21	4.63%
	The total number of strains	255	100%	454	100%

Unseparated data is represented by [N/A].

Table 2. Strains of ophiostomatalean fungi isolated from *Pinus massoniana* infested by *Monochamus alternatus* and *Bursaphelenchus xylophilus* in the current study.

Taxon	Species	Strain no	Location	GenBank no		
				ITS	TUB2	TEF1-α
1	*Ceratocystiopsis weihaiensis*	CFCC 55742 CXY4012	Huangyan	OK104016	OM103280	N/A
		CFCC 55743 CXY4013	Huangyan	OK104017	OM103281	N/A
		CXY4019	Huangyan	N/A	N/A	N/A
2	**Graphilbum xianjuensis** sp. nov.	**CFCC 55738ᵀ CXY4010**	Xianju	OK104014	OM103285	ON033177
		CFCC 55739 CXY4011	Xianju	OK104015	OM103286	ON033178
		CXY4018	Xianju	N/A	N/A	N/A
3	*Ophiostoma ips*	CFCC 55735 CXY4005	Xianju	OK104009	OM056673	N/A
		CFCC 55736 CXY4006	Xianju	OK104010	OM056674	N/A
		CFCC 55732 CXY4007	Xianju	OK104011	OM056675	N/A
4	**Ophiostoma taizhouense** sp. nov.	**CFCC 55740ᵀ CXC4001**	Huangyan	OK104005	OM103276	N/A
		CFCC 55731 CXY4002	Huangyan	OK104006	OM103277	N/A
		CFCC 55733 CXY4003	Huangyan	OK104007	OM103278	N/A
		CFCC 55734 CXY4004	Huangyan	OK104008	OM103279	N/A
5	*Sporothrix macroconidia*	CFCC 55741 CXY4009	Huangyan	OK104013	OL352730	N/A
		CXY4016	Huangyan	N/A	N/A	N/A
		CXY4017	Huangyan	N/A	N/A	N/A
6	*S. zhejiangensis*	CFCC 55737 CXY4008	Huangyan	OK104012	OM103282	N/A
		CXY4014	Huangyan	N/A	OM103283	N/A
		CXY4015	Huangyan	N/A	OM103284	N/A

Species names in bold are novel species described in this study. "T" indicates ex-type strains.
CFCC: China Forestry Culture Collection Center, Beijing, China.
CXY (Culture Xingyao): Culture collection of the Research Institute of Forest Ecology and Nature Conservation, Chinese Academy of Forestry.
Sequences missing data are indicated by [N/A]

Olympus microscope (Tokyo, Japan) with differential interference contrast. Fifty measurements were made for each microscopic taxonomical structure. The formula (min–) (mean–SD)–(mean+SD) (–max) was used to calculate averages, ranges, standard deviation (SD), minimum (min) and maximum (max) measurements, respectively. All relevant data pertaining to type specimens were deposited in MycoBank (www. MycoBank.org).

A 7 mm diameter mycelium plug was taken from a flourishing fungal colony using a sterile puncher and placed at the centre of 90 mm diameter 2% MEA plates, with one side of mycelium in contact with the media. Five replicate plates for each strain were incubated in a dark incubator at 5–35 °C with a temperature interval of 5 °C. The diameter of the colonies on each dish was measured every day by the orthogonal method until the fastest-growing mycelium reached the edge of the dish. The colony colour was then described using the Rayner (1970) colour chart.

DNA extraction, amplification and sequencing

Mycelia of representative strains were scraped with a sterile blade from the edge of the medium and transferred to 2 ml Eppendorf tubes for DNA extraction. DNA extraction and purification were carried out using the Invisorb Spin Plant Mini Kit (Tiangen, Beijing, China) according to the manufacturer's instructions. The primer pairs ITS1/ITS4 (White et al. 1990), BT2a/BT2b (Glass and Donaldson 1995) and EF1/EF2 (Jacobs et al. 2004) were used for the internal transcribed spacer (ITS) region of the nuclear ribosomal DNA operon, including spacers 1 and 2 and the 5.8S gene, the β-tubulin (BT) gene region and transcription elongation factor-1α (TEF-1α), respectively.

Polymerase chain reaction (PCR) amplification was performed using a Veriti 96-Well Fast Thermal Cycler (Applied Biosystems Veriti96, Foster City, CA, USA). PCR was carried out in a final volume of 25 μl (2.5 mM MgCl$_2$, 1× PCR buffer, 0.2 mM dNTP, 0.2 mM of each primer and 2.5 U Taq-polymerase enzyme). The cycling conditions were the same as those described for primer design (White et al. 1990; Glass and Donaldson 1995; Jacobs et al. 2004). The PCR products were purified using the MSB Spin PCR Apace Kit (250) (Invitek, Berlin, Germany) in accordance with the manufacturer's instructions.

Sequencing reactions were performed using a CEQ DTCS Quick Start Kit (Beckman Coulter, Brea, CA, USA) according to the manufacturer's instructions, with the same PCR primers as above. Nucleotide sequences were determined using a CEQ 2000 XL capillary automated sequencer (Beckman Coulter). Complementary and overlapping DNA electropherograms were checked and assembled using BioEdit v. 7.2.0. (Hall 1999).

Sequence alignment and phylogenetic analysis

Preliminary identification of the strains was conducted using the standard basic local alignment search tool (BLAST) searches in NCBI GenBank (http://blast.ncbi.nlm.nih.gov/Blast.cgi) and sequences with the highest similarity were downloaded from GenBank. Alignment of the genes was performed using MAFFT 7.0 (https://mafft.cbrc.jp/alignment/server/) (Katoh and Standley 2013), with the E-INS-I option with a gap-opening penalty of 1.53 and an offset value of 0.00 and edited manually using Molecular Evolutionary Genetic Analyses (MEGA) 7.0 software (Kumar et al. 2016).

Maximum Parsimony (MP), Maximum Likelihood (ML) and Bayesian Inference (BI) were used to infer the phylogenetic trees from each dataset. Two concatenated matrices of ITS and BT sequences were generated for *Ceratocystiopsis* and the *O. ips* complex.

MP analyses were implemented using PAUP* version 4.0b10 (Swofford 2003). The gaps were treated as the fifth base. Bootstrap analysis (1000 bootstrap repetitions) was used to determine the confidence level for inferring the nodes in the tree topology. Tree bisection and reconnection were selected as the branch swapping option. For each dataset of the 5000 most-parsimonious trees, the best tree that was automatically output by PAUP* v. 4.0b10 was selected for use in the figure.

ML analyses were carried out using RAxML-HPC (version 8.2.3; Stamatakis 2014) and the selected GTR-GAMMA model of site substitution included the estimation of gamma-distributed rate heterogeneity and a proportion of invariant sites. ML analysis included 1000 bootstrap analyses to evaluate the overall reliability of the node support value and tree topology.

BI analyses using Markov Chain Monte Carlo (MCMC) methods were implemented in MrBayes version 3.1.2 (Ronquist et al. 2012), from a random starting tree for 5,000,000 generations, to calculate posterior probability values for the nodes. When we run to 5,000,000 generations, the split frequencies of all datasets were less than 0.01. Chain convergence for all datasets was determined using Tracer 1.7 (Rambaut et al. 2018). No lack of convergence was detected. Trees were sampled every 100 generations and the first 25% of trees sampled were discarded as burn-in, while the remaining trees were used to calculate Bayesian posterior probabilities of the clades. Phylogenetic trees were edited in Figtree version 1.4.3 (http://tree.bio.ed.ac.uk/sosftware/figtree/) and Adobe Illustrator CS6.

Results

Fungal isolation and sequence comparison

A total of 709 strains of fungi were isolated from the *M. alternatus* larval galleries and pupal chambers (2nd–5th instars). The strains were divided into 18 taxa, based on colony morphology and multi-locus DNA sequence alignment (ITS and BT) analysis. A total of 255 fungal strains, representing 14 taxa, were isolated from the galleries of 2nd–3rd instar larvae. Taxon 4 was the dominant taxon accounting for 62 of the 255 strains. A total of 454 fungal strains were isolated from the galleries and pupal chambers of the 4th–5th instar larvae and divided into six taxa. The dominant taxon was *O. ips*, accounting for 231 out of the 454 strains (Table 1). Only two fungi (*Diplodia sapinea* and *Penicillium* sp.) could be isolated from both 2nd–3rd instar larval galleries and 4th–5th instar larval galleries and pupal chambers, except for unidentified species. In this study, 320 ophiostomatalean fungi strains (320 strains out of 709 fungal strains) were isolated, including six tentative species. Four
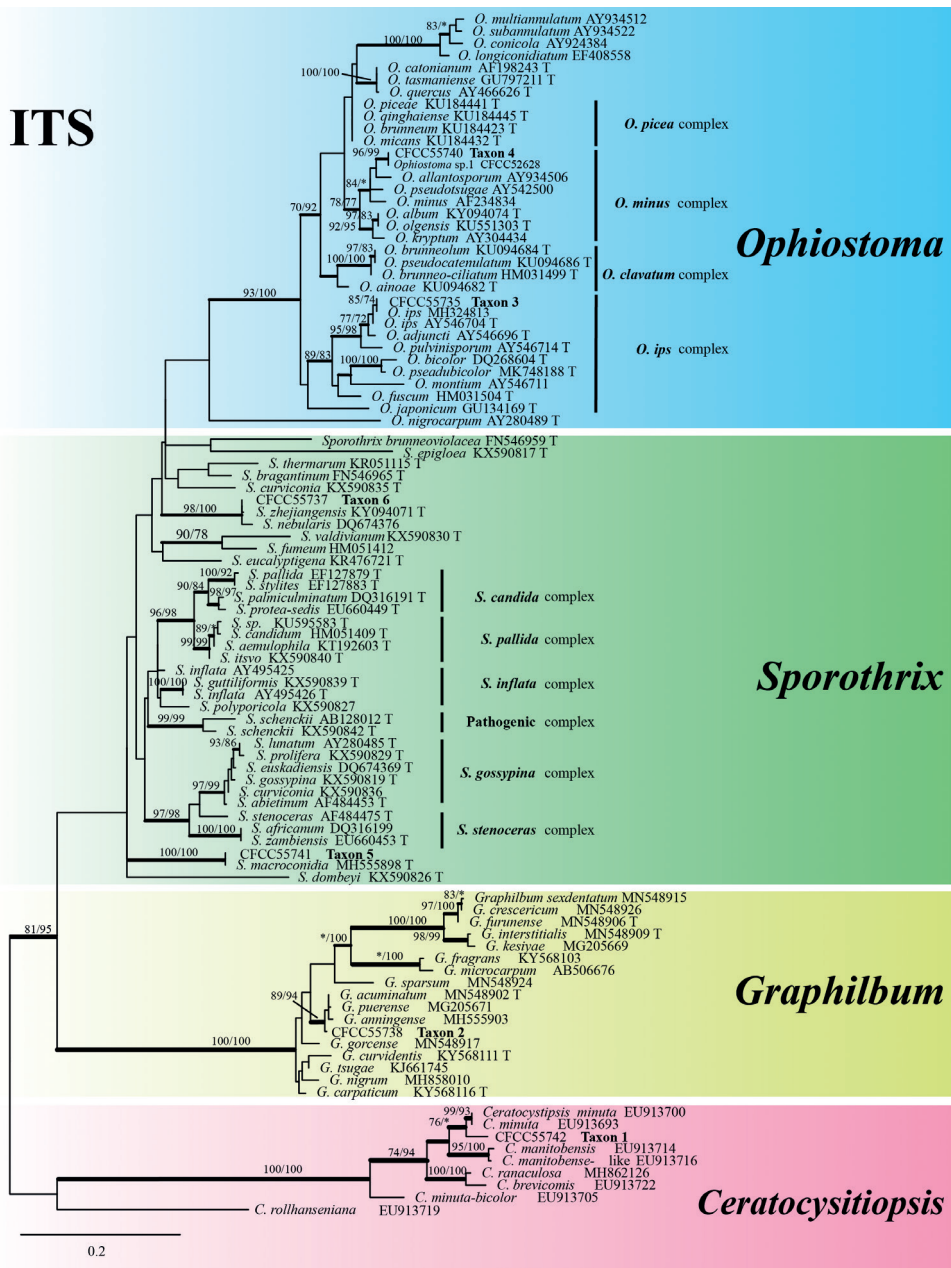
Figure 1. ML tree of the ITS region of *Ophiostoma*, *Sporothrix*, *Graphilbum*, *Ceratocystiopsis*. Bootstrap values of ML/MP ≥ 70% are recorded at nodes as ML/MP and bold branches indicate posterior probability values ≥ 0.9. ML and MP, Bootstrap values < 70% are indicated by the symbol *. The tree is drawn to scale (see bar) with branch length measured in the number of substitutions per site. Strains representing ex-type sequences are marked with "T." ML, Maximum Likelihood; MP, Maximum Parsimony; BI, Bayesian Inference and the final alignment of 734 positions, including gaps.

of these six species were obtained from the galleries of the 2nd–3rd instar larvae and two species were isolated from the galleries and pupal chambers of the 4th–5th instar larvae (Table 1).

Phylogenetic analyses

There were 709 strains obtained in this study, but some strains have a small number of strains. In this study, we selected 2–4 representative strains from each Taxon and nineteen representative strains of Ophiostomatales belonging to six tentative species (Taxa 1–6) were selected for phylogenetic analyses (Table 2). All the sequences used for the phylogenetic trees were submitted to GenBank. The three phylogenetic approaches yielded similar topologies, with statistical support varying slightly for each sequence dataset. Phylograms derived from ML analysis were presented
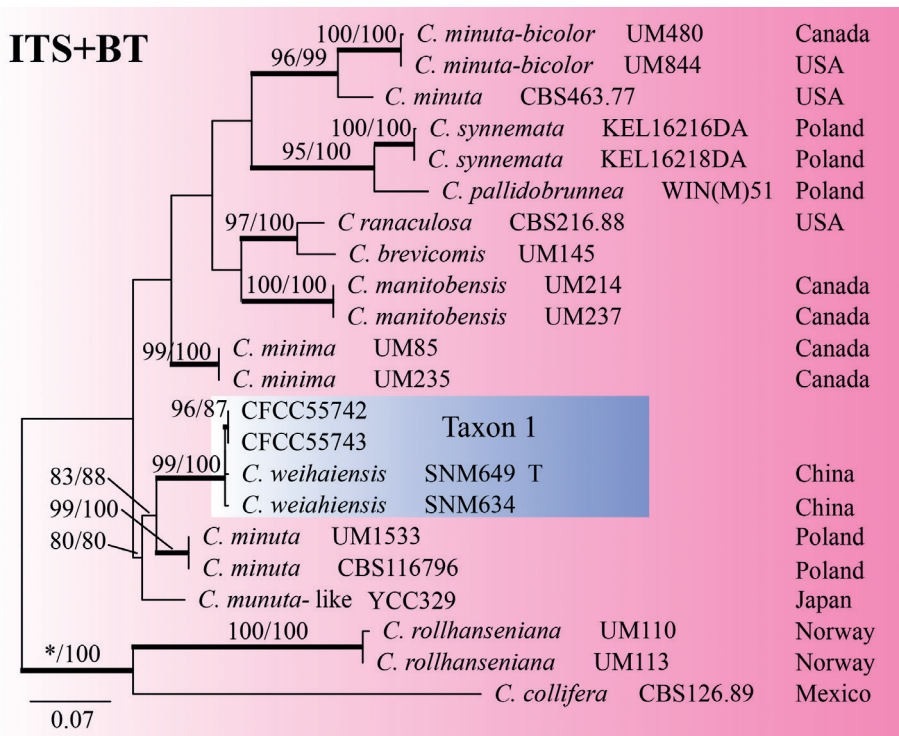
Figure 2. ML tree of *Ceratocystiopsis* generated from the combined (ITS+BT) sequence data. Bootstrap values of ML/MP ≥ 70% are recorded at nodes as ML/MP and bold branches indicate posterior probability values ≥ 0.9. ML and MP, Bootstrap values < 70% are indicated by the symbol *. The tree is drawn to scale (see bar) with branch length measured in the number of substitutions per site. Strains representing ex-type sequences are marked with "T." Abbreviations: ML, Maximum Likelihood; MP, Maximum Parsimony; BI, Bayesian Inference and the final alignment of 1040 positions, including gaps.
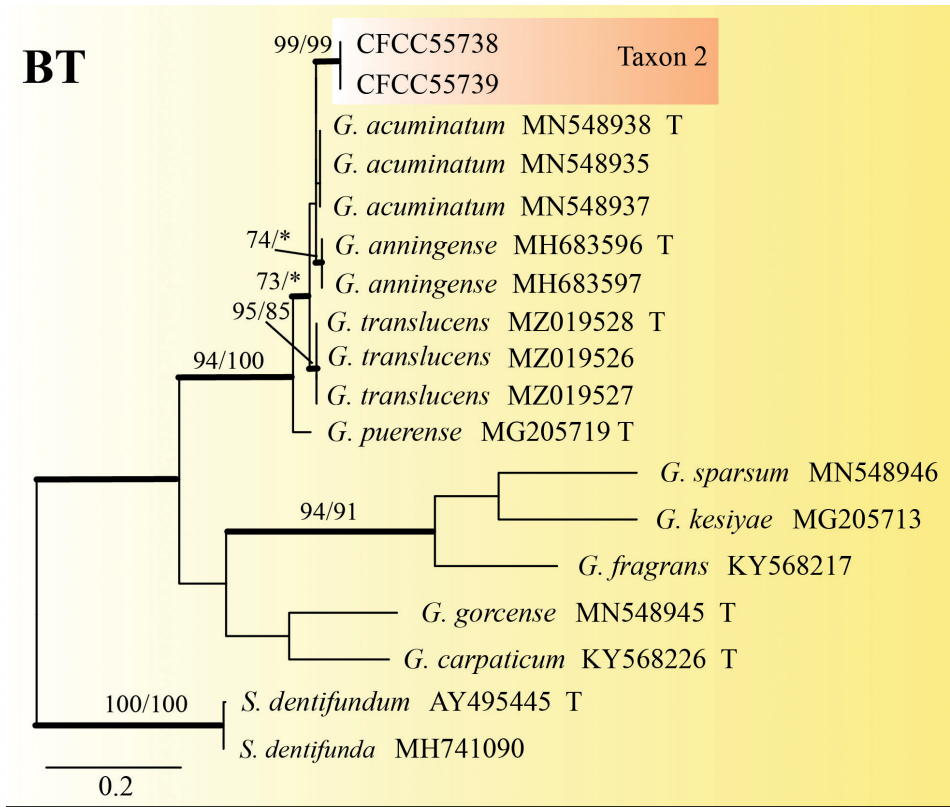
Figure 3. ML tree of the BT region of *Graphilbum*. Bootstrap values of ML/MP ≥ 70% are recorded at nodes as ML/MP and bold branches indicate posterior probability values ≥ 0.9. ML and MP, Bootstrap values < 70% are indicated by the symbol *. The tree is drawn to scale (see bar) with branch length measured in the number of substitutions per site. Strains representing ex-type sequences are marked with "T." Abbreviations: ML, Maximum Likelihood; MP, Maximum Parsimony; BI, Bayesian Inference and the final alignment of 548 positions, including gaps.

for each individual dataset, along with nodal supports derived from the MP and BI analyses.

The ITS phylogenetic tree showed that six representative taxa (Table 2) belonged to six phylogenetic clades (Fig. 1). Taxa 1–2 nested within the *Ceratocystiopsis* and *Graphilbum* lineages, respectively; Taxa 3–4 nested within the *Ophiostoma* lineage, Taxon 3 belonging to the *Ophiostoma minus* complex and Taxon 4 belonging to the *O. ips* complex (de Beer and Wingfield 2013); Taxa 5–6 belonged to the *Sporothrix* and were not placed in any complex defined by de Beer et al. (2016) (Fig. 1).

Taxon 1 included three isolates, all of which were included in the analyses (Tables 1, 2). Based on the phylogenetic analysis of the combined dataset (ITS+BT), this taxon forms a well-supported clade with *Ceratocystiopsis weihaiensis* (Fig. 2). Hence, the strains in Taxon 1 should be identified as *C. weihaiensis*.
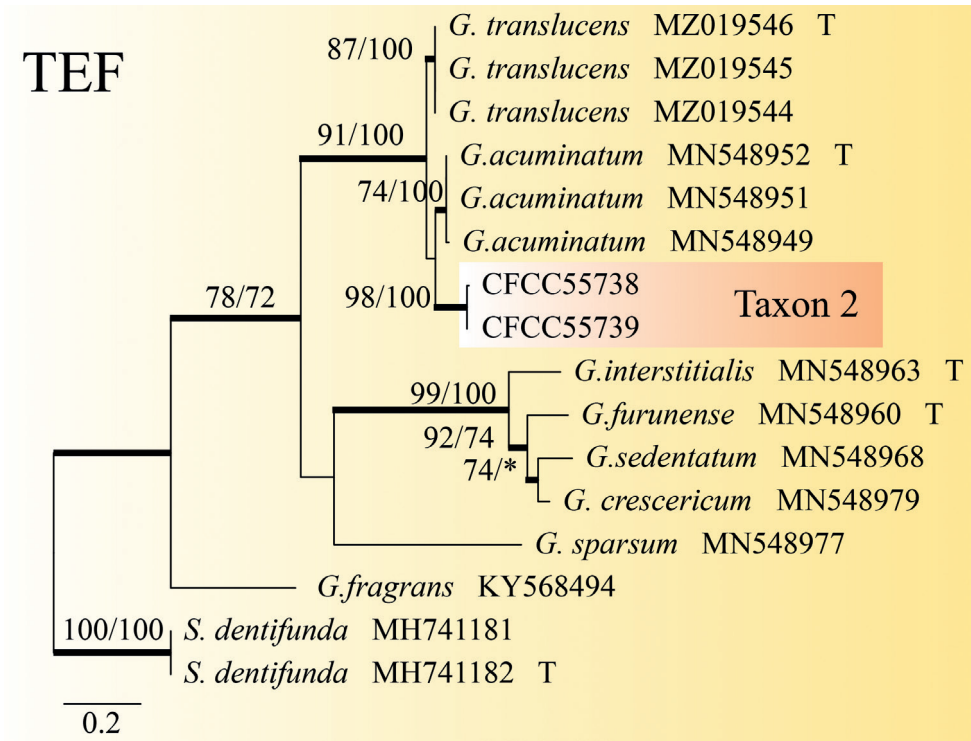
Figure 4. ML tree of the TEF region of *Graphilbum*. Bootstrap values of ML/MP ≥ 70% are recorded at nodes as ML/MP and bold branches indicate posterior probability values ≥ 0.9. ML and MP, Bootstrap values < 70% are indicated by the symbol *. The tree is drawn to scale (see bar) with branch length measured in the number of substitutions per site. Strains representing ex-type sequences are marked with "T." Abbreviations: ML, Maximum Likelihood; MP, Maximum Parsimony; BI, Bayesian Inference and the final alignment of 725 positions, including gaps.

Taxon 2 consisted of 12 isolates, three of which were used for phylogenetic analyses (Tables 1, 2). The phylograms of ITS, BT and TEF-1α datasets revealed that Taxon 2 was an independent clade closely related to *Graphilbum acuminatum*, *G. anningense* and *G. translucens* (Figs 1, 3, 4). As a result, Taxon 2 should be interpreted as belonging to a distinct, undescribed *Graphilbum* species.

Taxon 3 was represented by three sequences that formed a well-supported clade with *O. ips*, based on the ITS tree (Fig. 1). Further phylogenetic analysis, based on combined datasets (ITS+BT) yielded similar results (Fig. 5). Based on ITS and BT phylogenetic analysis, Taxon 4, represented by three sequences, has a well-supported independent clade with *Ophiostoma* sp.1 (CFCC52628) (Wang et al. 2019), which is closely related to *O. allantosporum*, *O. pseudotsugae* and *O. wuyingensis* (Figs 6, 7). Thus, Taxon 3 should be identified as a known species of *O. ips*, whereas Taxon 4 should be interpreted as a distinct, undescribed *Ophiostoma* species.
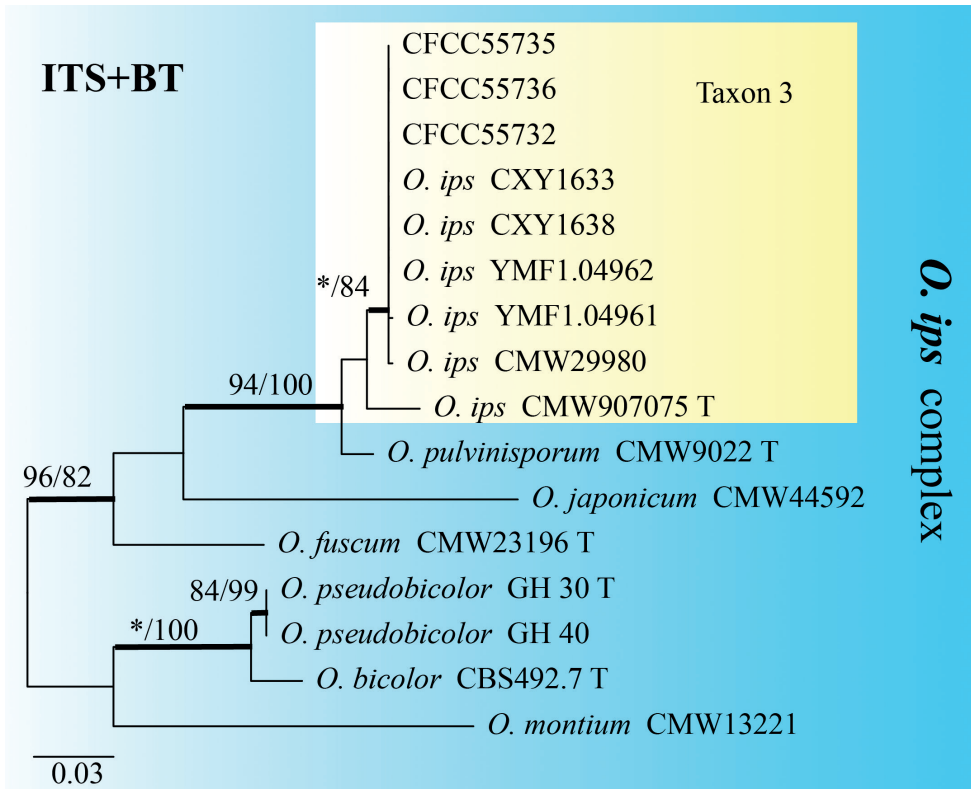
Figure 5. ML tree of the *O. ips* complex generated from the combined (ITS+BT) sequence data. Bootstrap values of ML/MP ≥ 70% are recorded at nodes as ML/MP and bold branches indicate posterior probability values ≥ 0.9. ML and MP, Bootstrap values < 70% are indicated by the symbol *. The tree is drawn to scale (see bar) with branch length measured in the number of substitutions per site. Strains representing ex-type sequences are marked with "T." Abbreviations: ML, Maximum Likelihood; MP, Maximum Parsimony; BI, Bayesian Inference and the final alignment of 953 positions, including gaps.

Taxon 5 consisted of four isolates, three of which were used for the phylogenetic analyses. Based on the ITS and BT phylogenetic trees, Taxon 5 grouped with *Sporothrix zhejiangensis* (Figs 1, 8). Thus, it should be identified as *S. zhejiangensis*.

Taxon 6 consisted of eight isolates, three of which were selected for analysis. Taxon 6 grouped with *Sporothrix macroconidia*, based on the ITS and BT phylogenetic trees (Figs 1, 8). As a result, Taxon 6 was designated as *S. macroconidia*.

Taxonomy

According to the ITS and BT phylogenetic analyses, six different taxa (Taxon 1–6) were identified in this study. They represent four known species, *Ceratocystiopsis weihaiensis*, *O. ips*, *S. macroconidia* and *S. zhejiangensis* (Lun et al. 2019; Wang et al. 2019; Chang et al. 2021), in addition to two novel species. They are described as follows:
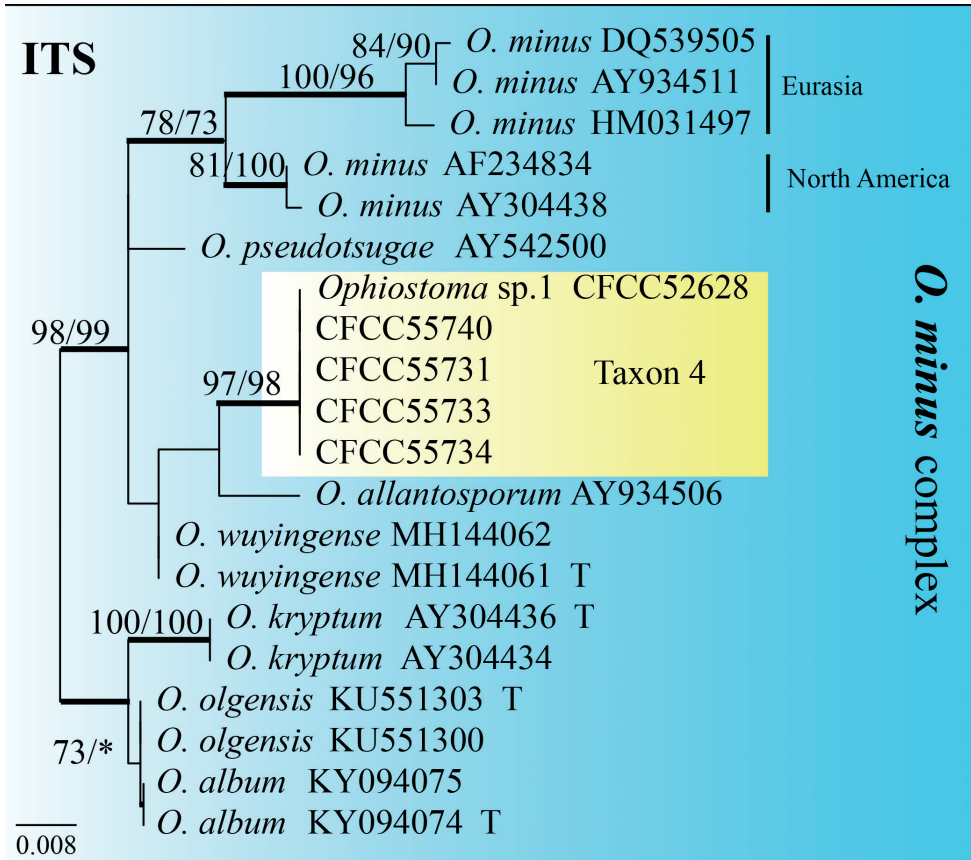
Figure 6. ML tree of the ITS region of *O. minus* complex. Bootstrap values of ML/MP ≥ 70% are recorded at nodes as ML/MP and bold branches indicate posterior probability values ≥ 0.9. ML and MP, Bootstrap values < 70% are indicated by the symbol *. The tree is drawn to scale (see bar) with branch length measured in the number of substitutions per site. Strains representing ex-type sequences are marked with "T." Abbreviations: ML, Maximum Likelihood; MP, Maximum Parsimony; BI, Bayesian Inference and the final alignment of 537 positions, including gaps.

Graphilbum xianjuensis G. H. Zheng & Q. Lu, sp. nov.
MycoBank No: 842387
Fig. 9

Etymology. The epithet *xianju* (Latin) refers to the type locality.

Type. CHINA, Zhejiang, Xianju County, from *Monochamus alternatus* galleries and pupal chambers of *Pinus massoniana* infested by *Bursaphelenchus xylophilus*, December 2020, collected by G. H. Zheng, culture ex-holotype CFCC55738 = CXY4010.

Description. Sexual morph: not observed.

Asexual form: *Hyalorhincladiella*-like. Conidiogenous cells were simple or loosely branched, (9.12–) (15.44) – (48.64) (–62.49) × (1.25–) (1.53) – (2.21) (–2.45) μm. Co-
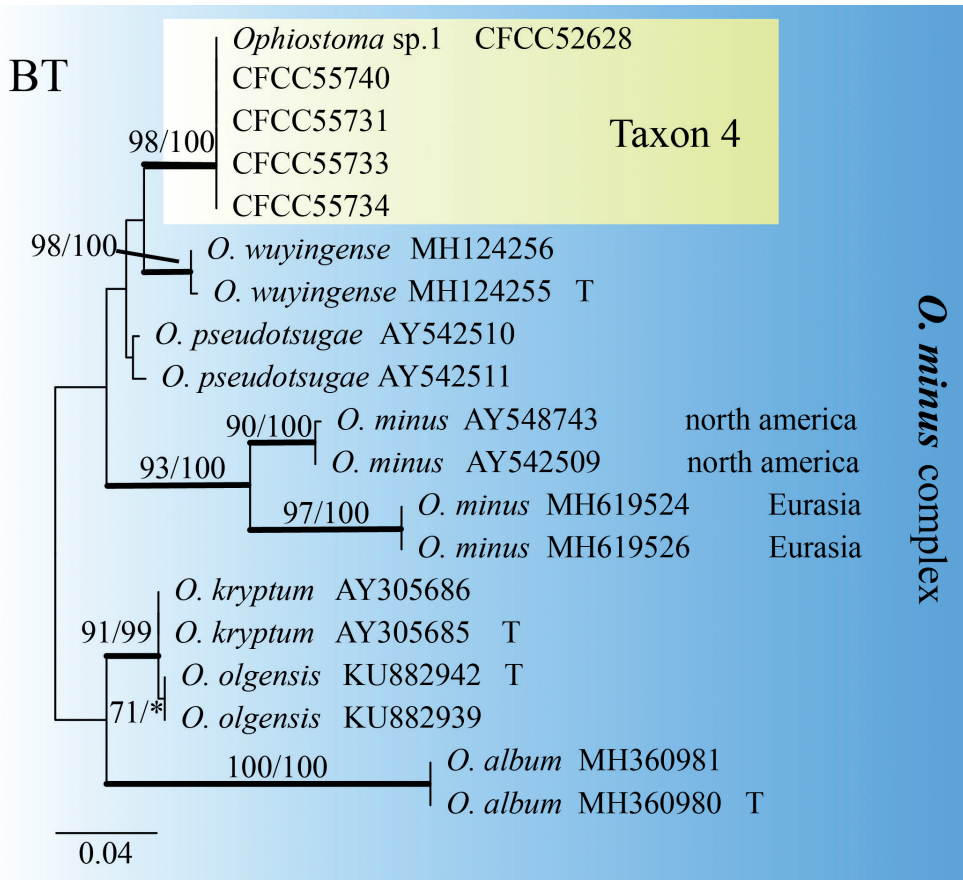
Figure 7. ML tree of the BT region of *O. minus* complex. Bootstrap values of ML/MP ≥ 70% are recorded at nodes as ML/MP and bold branches indicate posterior probability values ≥ 0.9. ML and MP, Bootstrap values < 70% are indicated by the symbol *. The tree is drawn to scale (see bar) with branch length measured in the number of substitutions per site. Strains representing ex-type sequences are marked with "T." Abbreviations: ML, Maximum Likelihood; MP, Maximum Parsimony; BI, Bayesian Inference and the final alignment of 495 positions, including gaps.

nidia hyaline, smooth, cylindrical, aseptate, (4.76–) (6.07) – (9.87) (–13.41) × (0.99 –) (1.32) – (2.1) (–2.65) μm.

Culture characteristics. Colonies on 2% MEA reaching 44.9 mm diameter, after incubation in the dark at 25 °C for 3 d, growth rate up to 14.98 mm/d at the fastest and colony margin irregular. Mycelium superficial to flocculose or floccose, hyaline, reverse grey-white. The optimal temperature for growth at 30 °C; no growth was observed at 5 °C.

Habitat and distribution. Larval galleries and pupal chambers of *Monochamus alternatus* in *Pinus massoniana*, infested by *Bursaphelenchus xylophilus*, in Zhejiang Province, China.
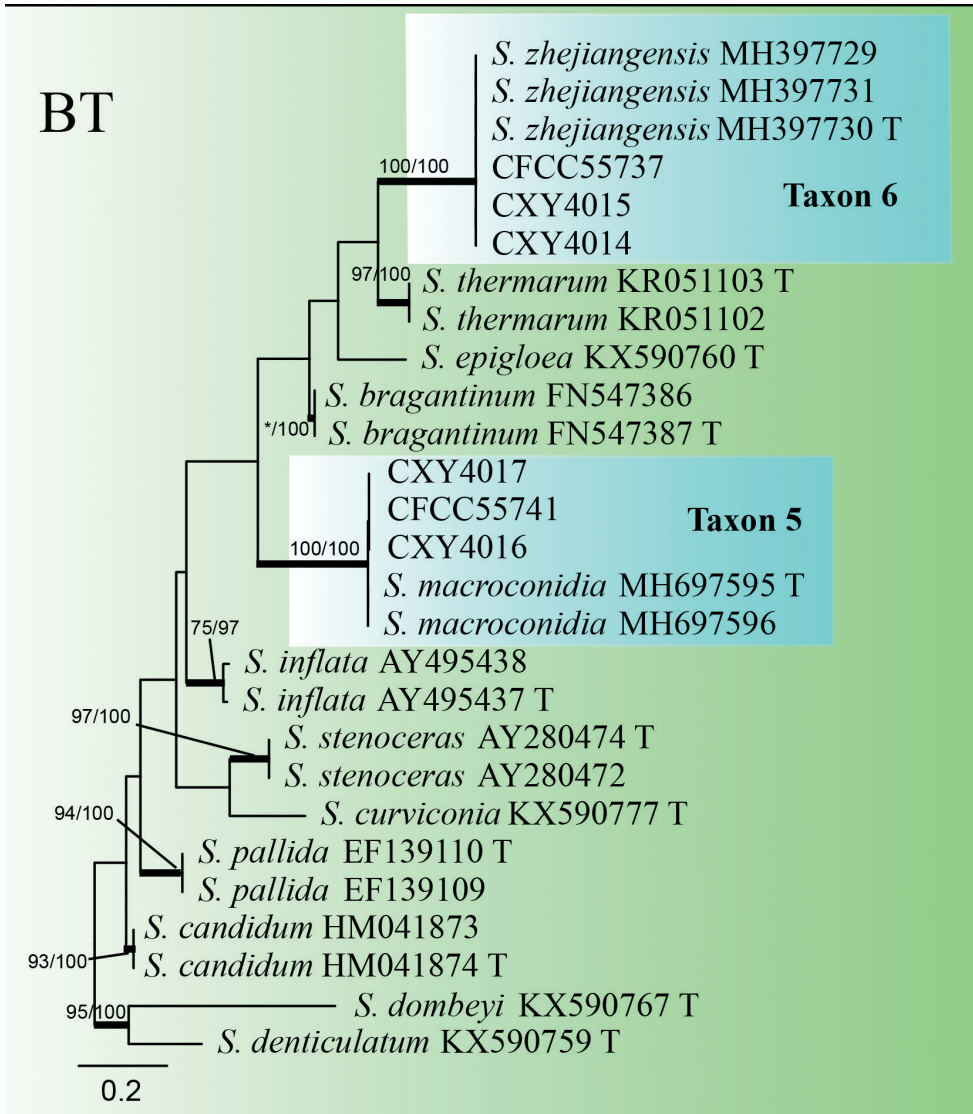
BT

Figure 8. ML tree of *Sporothrix* generated from the BT sequence data. Bootstrap values of ML/MP ≥ 70% are recorded at nodes as ML/MP and bold branches indicate posterior probability values ≥ 0.9. ML and MP, Bootstrap values < 70% are indicated by the symbol *. The tree is drawn to scale (see bar) with branch length measured in the number of substitutions per site. Strains representing ex-type sequences are marked with "T." Abbreviations: ML, Maximum Likelihood; MP, Maximum Parsimony; BI, Bayesian Inference and the final alignment of 313 positions, including gaps.

Additional specimens examined. CHINA, Zhejiang, from *Monochamus alternatus* galleries and pupal chambers of *Pinus massoniana* infested by *Bursaphelenchus xylophilus*, December 2020, collected by G. H. Zheng, CFCC55739 = CXY4011, CXY4018.
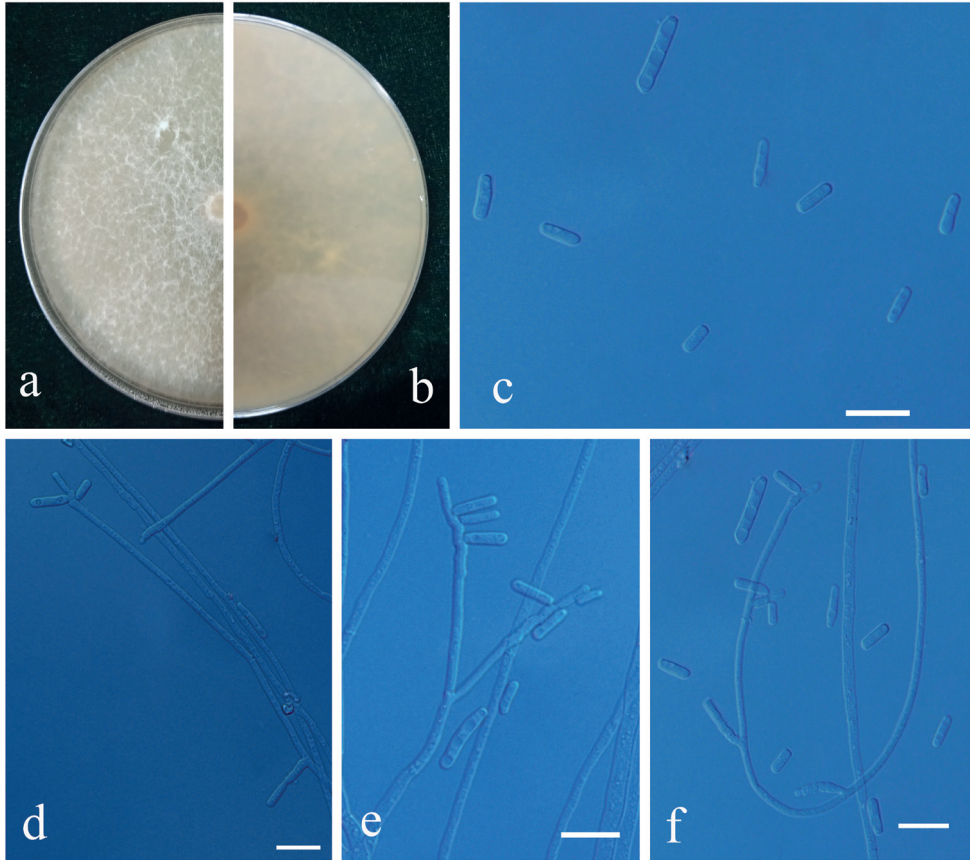
Figure 9. Morphological characteristics of *Graphilbun xianjuensis* sp. nov. (CFCC = 55738, Taxon 2). **a, b** thirty-day-old cultures on 2% MEA **c–f** *Hyalorhincladiella*-like asexual morph: conidiogenous cells and conidia. Scale bars: 10 μm (**c–f**).

Note. Only the *Hyalorhincladiella*-like asexual form was observed in *Graphilbum xianjuensis*. This is closely related to *the G. acuminatum*, *G. anningense* and *G. translucens*, based on the ITS, BT and TEF1-α phylogenetic trees (Figs 1, 3, 4). Four species differed according to the size of their conidia. The conidia of *G. xianjuensis* (6.07–9.87 μm) are longer than those of *G. anningense* (4.5–6.4 μm), *G. acuminatum* (3.5–6 μm) and *G. translucens* (2.4–3.5 μm) (Wang et al. 2019; Jankowiak et al. 2020). Besides, *G. xianjuensis* was found to be associated with *M. alternatus* and PWN-infested *P. massoniana*, whereas *G. anningense* was reported in galleries of *T. yunnanensis* and *T. minor* associated with *P. yunnanensis* in southwest China (Wang et al. 2019), *G. acuminatum* has been reported in galleries of *Ips acuminatus* and *Pityogenes bidentatus* associated with *P. sylvestris* in Europe (Jankowiak et al. 2020) and *G. translucens* was first reported in *Cryphalus piceae* associated with *P. densiflora*. In conclusion, four species of *Graphilbum* differ not only in geographical distribution, but also in hosts and vectors. The optimum

growth temperature of *G. xianjuensis*, *G. anningense* and *G. translucens* is 30 °C and only *G. acuminatum* had an optimum growth temperature of 25 °C (Wang et al. 2019; Jankowiak et al. 2020).

Ophiostoma taizhouense G. H. Zheng & Q. Lu, sp. nov.
MycoBank No: 842388
Fig. 10

Etymology. '*taizhou*' (Latin) refers to the type locality.

Type. China, Zhejiang Province, Taizhou City, from *Monochamus alternatus* galleries of *Pinus massoniana* infested by *Bursaphelenchus xylophilus*, October 2020, collected by G. H. Zheng and Q. Lu, culture ex-holotype CFCC55740 = CXY4001.

Description. Sexual morph: not observed.

Asexual form: *Hyalorhincladiella*-like. Conidiophores abundant, conidiogenous cells single, disposed in a dense rachis (3.08–) (6.6) – (15.63) (–23.07) × (1.11–) (1.44) – (2.23) (–2.9) μm. Conidia hyaline, smooth, lunate, ellipsoid
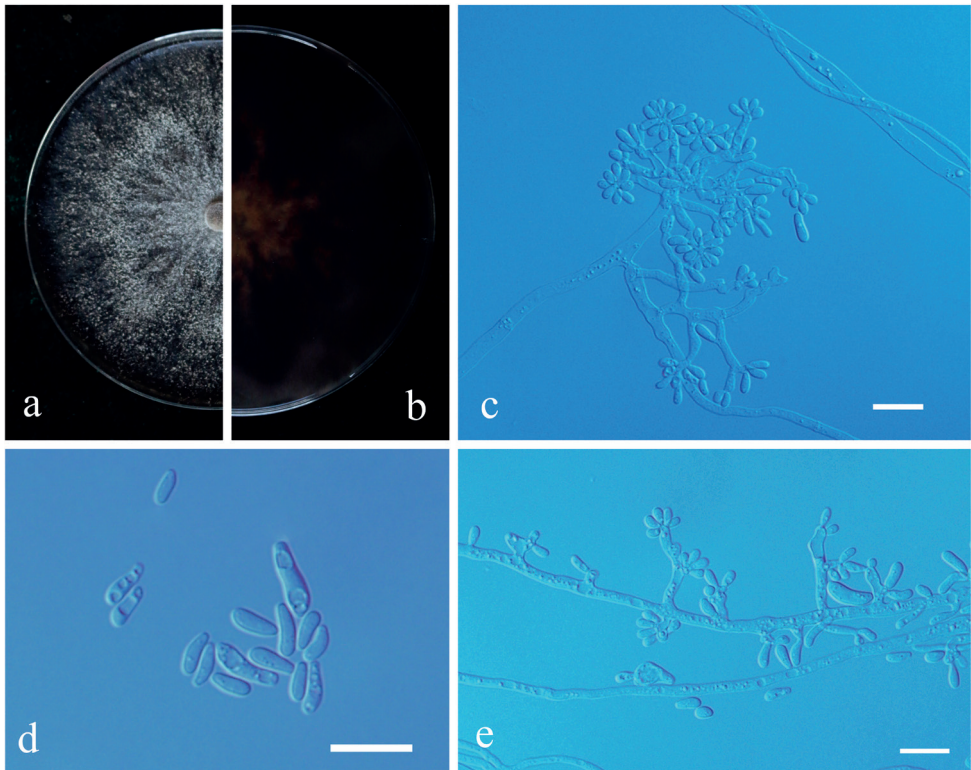

Figure 10. Morphological characteristics of *Ophiostoma taizhouense* sp. nov. (CFCC = 55740, Taxon 4). **a, b** twenty-day-old cultures on 2% MEA **c–e** *Hyalorhincladiella*-like asexual morph: conidiogenous cells and conidia. Scale bars: 10 μm (**c–e**).

to ovoid, curvulate, aseptate, (3.24–) (4.27) – (7.42) (–10.08) × (1.17–) (1.6) – (2.39) (–2.86) μm.

Culture characteristics. Colonies on 2% MEA reaching 62.5 mm diameter, after incubation in the dark at 25 °C for 3 d, growth rate up to 22.83 mm/d at the fastest, colony margin smooth, hyphae are superficial on agar. Some white mycelium was produced early during growth and became black after 8–15 d, transitioning from brown to dark brown. The optimal temperature for growth at 30 °C; no growth was observed at 5 °C.

Habitat and distribution. Larval galleries of *Monochamus alternatus* in *Pinus massoniana*, infested by *Bursaphelenchus xylophilus*, in Zhejiang Province, China.

Additional specimen examined. China, Zhejiang, Taizhou City, from *Monochamus alternatus* galleries of *Pinus massoniana* infested by *Bursaphelenchus xylophilus*, October 2020, collected by G. H. Zheng and Q. Lu, CFCC55731 = CXY4002, CFCC55733 = CXY4003, CFCC55734 = CXY4004.

Note. Only the *Hyalorhincladiella*-like asexual form was observed in *Ophiostoma taizhouense*. According to ITS and BT phylogenetic analysis, it has a well-supported independent clade with *Ophiostoma* sp.1 (CFCC52628) and is closely related to *O. allantosporum*, *O. pseudotsugae* and *O. wuyingensis* (Figs 1, 5, 6). Only one strain of *Ophiostoma* sp.1 was isolated in our laboratory from *P. yunnanensis* infested with *T. yunnanensis* in Yunnan Province, so this strain was not officially named before this study. Although the geographical location and host of *O. taizhouense* and *Ophiostoma* sp.1 are different, their culture characteristics and gene sequences (ITS and BT) are identical (Figs 1, 5, 6) (Wang et al. 2019). In general, the conidia of *O. taizhouense* (4.27–7.42 μm) are longer than those of *O. minus* (2.5–6 μm) (Upadhyay 1981) and *O. pseudotsugae* (2.7–5 μm) (Rumbold 1936). The optimal growth temperature of *O. allantosporum* and *O. pseudotsugae* was 25 °C, that of *O. wuyingensis* was 25–30 °C and that of *O. taizhouense* was 30 °C (Gorton and Webber 2000, Chang et al. 2019). Both *O. wuyingensis* and *O. taizhouense* showed pigmentation on 2% MEA medium, whereas *O. allantosporum* has mid-brown hyphae, *O. pseudotsugae* has white-grey to snuff-brown, both showed no agar pigmentation (Rumbold 1936; Villarreal et al. 2005). *Ophiostoma wuyingensis* was first isolated from the gallery of *Ips typographus* on *P. koraiensis* in Heilongjiang Province (Chang et al. 2019). *Ophiostoma allantosporum* and *O. pseudotsugae* were isolated from *P. resinosa* in the USA and *P. menziesii* were infected with *Dendroctonus frontalis* in North America (Gorton and Webber 2000). Strains of *O. taizhouense* in this study were isolated from *P. massoniana* infected with PWN and *M. alternatus*.

Discussion

In the current study, 255 (containing 14 species) and 454 (containing six species) strains were obtained from *M. alternatus* larval galleries and pupal chambers of 2nd–3rd and 4th–5th instar, respectively, in *P. massoniana* infested with PWN in the Zhejiang Province, south-eastern China (Table 1). A total of 320 ophiostomatalean fungal strains out of overall 709 strains were obtained. The fungal diversity of 2nd–3rd

instar larvae was higher than that of 4th–5th instar larvae (Table 1; Fig. 11). *Ophiostoma taizhouense* is the dominant species in the 2nd–3rd instar and *O. ips* is the primary species at the 4th–5th instar. This is both similar and distinct from the previous research. Some studies found *Trichoderma* sp. or *Sporothrix* sp.1 to be the most common fungus associated with PWD (Zeng et al. 2006; Zhao et al. 2013), while others found the same to be *O. ips* (Lun et al. 2019), as was found here. The phenomenon could be caused by fungal succession, which occurs when PWN and *M. alternatus* select fungal companions that are more conducive to their own growth and reproduction at different life cycle stages. Therefore, future research on fungal diversity and abundance will necessitate a more comprehensive sampling analysis.

Only two common fungal species were obtained from both 2nd–3rd instar larval galleries, 4th–5th instar larval galleries and pupal chambers. The abundance of *D. sapinea* (103 out of 709) was higher than that of *Penicillium* sp. (7 out of 709). *Diplodia sapinea* is commonly isolated from *P. nigra* tip blight, *P. halepensis* and *P. pinaster* branch cankers worldwide (Luchi et al. 2014). It is an important pathogen of the *Pinus* spp. In addition, research has shown that *D. sapinea* can promote PWN reproduction and settlement (Kobayashi et al. 1974; Sriwati et al. 2007). *Penicillium* sp. is a common fungus in nature that also serves as an important biocontrol fungus (Sartaj et al. 2011; Win et al. 2021). However, there are no reports of *Penicillium* sp. affecting PWN, either negatively or positively.

Ophiostoma ips was first reported in pine trees associated with bark beetles in the south-eastern United States (Rumbold 1936) and it has since been confirmed, using
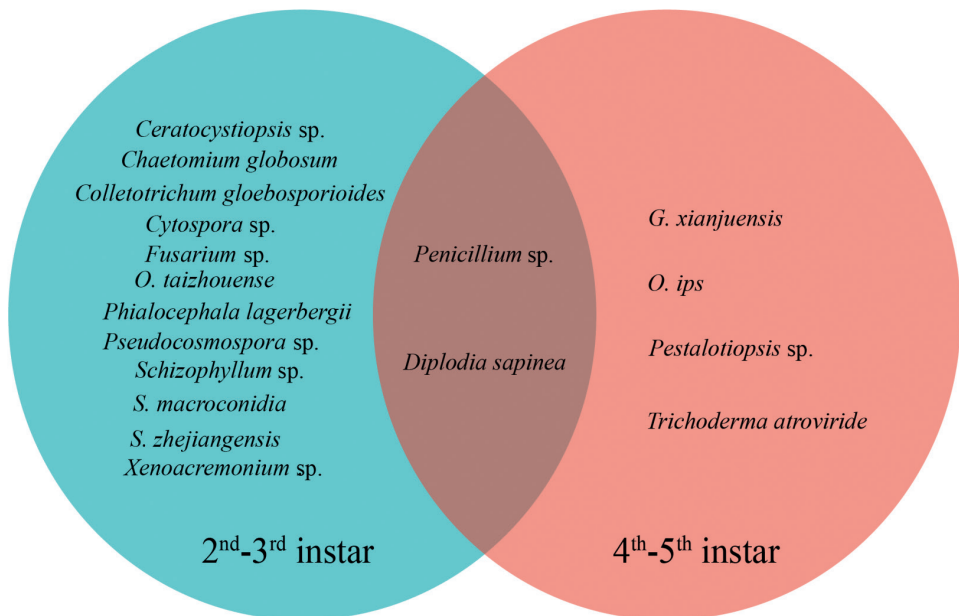

Figure 11. Diagram showing the species of fungi were isolated from the galleries and pupae chambers of different instar larvae of *Monochamus alternates*.

microsatellite markers, to be distributed worldwide (Zhou et al. 2007). Unfortunately, the study did not include Chinese strains. However, *O. ips* is regarded as one of the most stable natural associates of PWN in the wild of China (Zhao et al. 2013; Lun et al. 2019). According to Lun et al. (2019), *O. ips* was the dominant strain associated with PWN and was frequently isolated at the late stage of PWD. In a study by Zhao et al. (2013), *O. ips* was one of the three dominant ophiostomatoid fungi associated with PWN, with an isolation rate of 36%. Although *O. ips* was not found in the galleries of *M. alternatus* 2nd–3rd instar larvae in this study, it was the primary species at the 4th–5th instar, with an isolation rate of 50.88% and fungal abundance was much higher than that of other fungi during this period. Experiments with nematode propagation revealed that *O. ips* could breed nematodes, but not as effectively as *Botrytis cinerea* (Pimentel et al. 2021). In addition, biochemical analysis results revealed that *O. ips* could produce a wide range of volatile chemical substances (Cale et al. 2019). The 4th–5th instar larvae of *M. alternatus* are closely related to pinewood nematode dispersal stage J_{IV} (the fourth-stage dispersal juvenile). However, the mechanism underlying the interaction between *O. ips* and dispersal nematode juveniles is still lacking.

Ophiostoma taizhouense was the second most frequently isolated species of ophiostomatalean fungi in our study (62 out of the 255 strains); nevertheless, it was only associated with 2nd–3rd instar larvae. The association between *O. taizhouense* and PWD needs further experimental verification as a new species. Although the isolation rate of *Phialocephala* sp. and *Xenoacremonium* sp. is relatively high in 2nd–3rd instar larvae, these two fungi are both endophytes and there are no reports relating them to PWD.

In addition, three known ophiostomatalean fungi (*C. weihaiensis*, *S. macroconidia* and *S. zhejiangensis*) and one new species (*G. xianjuensis*) were revealed with low isolation rates during the survey. Simultaneously, some common endophytic and saprophytic fungi were isolated from the galleries and pupal chambers of *M. alternatus* larvae. The relationship between these fungi and PWN has not yet been reported.

In this study, a relatively large diversity of fungal species was obtained and identified as associated with PWN and *M. alternatus* in south-eastern China. The results showed that the fungal diversity and abundance of the 2nd–3rd instar larvae differed from those of the 4th–5th instar larvae. Fungi play an important role during the successful survival, reproduction and spread of PWN (Zhao et al. 2014; Zhao and Sun 2017). Hence, it is vital to explore the relationship between fungi and PWDs. This study provides a research basis for the fungi-PWN-*M. alternatus* symbiosis.

Acknowledgements

References

Abelleira A, Picoaga A, Mansilla JP, Aguin O (2011) Detection of *Bursaphelenchus xylophilus*, causal agent of pine wilt disease on *Pinus pinaster* in Northwestern Spain. Plant Disease 95(6): 776–776. https://doi.org/10.1094/PDIS-12-10-0902

Cale JA, Ding R, Wang F, Rajabzadeh R, Erbilgin N (2019) Ophiostomatoid fungi can emit the bark beetle pheromone verbenone and other semiochemicals in media amended with various pine chemicals and beetle-released compounds. Fungal Ecology 39: 285–295. https://doi.org/10.1016/j.funeco.2019.01.003

Chang R, Duong TA, Taerum SJ, Wingfield MJ, Zhou X, Yin M, de Beer ZW (2019) Ophiostomatoid fungi associated with the spruce bark beetle *Ips typographus*, including 11 new species from China. Persoonia. Molecular Phylogeny and Evolution of Fungi 42(1): 50–74. https://doi.org/10.3767/persoonia.2019.42.03

Chang RL, Zhang XY, Si HL, Zhao GY, Yuan XW, Liu TT, Bose T, Dai MX (2021) Ophiostomatoid species associated with pine trees (*Pinus* spp.) infested by *Cryphalus piceae* from eastern China, including five new species. MycoKeys 83: 181–208. https://doi.org/10.3897/mycokeys.83.70925

Cheng XY, Tian XL, Wang YS, Lin RM, Mao ZC, Chen NS, Xie BY (2013) Metagenomic analysis of the pinewood nematode microbiome reveals a symbiotic relationship critical for xenobiotics degradation. Scientific Reports 3(1): e1869. https://doi.org/10.1038/srep01869

de Beer ZW, Wingfield MJ (2013) Emerging lineages in the Ophiostomatales. In: Seifert KA, de Beer ZW, Wingfield MJ (Eds) The Ophiostomatoid Fungi: Expanding Frontiers. CBS-KNAW Fungal Biodiversity Centre, Utrecht, The Netherlands 21–46.

de Beer ZW, Duong TA, Barnes I, Wingfield BD, Wingfield MJ (2014) Redefining Ceratocystis and allied genera. Studies in Mycology 79(1): 187–219. https://doi.org/10.1016/j.simyco.2014.10.001

de Beer ZW, Duong TA, Wingfield MJ (2016) The divorce of *Sporothrix* and *Ophiostoma*: Solution to a problematic relationship. Studies in Mycology 83(1): 165–191. https://doi.org/10.1016/j.simyco.2016.07.001

de Beer ZW, Procter M, Wingfield MJ, Marincowitz S, Duong TA (2022) Generic boundaries in the Ophiostomatales reconsidered and revised. Studies in Mycology 101: 57–120. https://doi.org/10.3114/sim.2022.101.02

Eckhardt LG (2002, November) *Leptographium* Species: Tree Pathogens, Insect Associates, and Agents of Blue-Stain. Forest Science 48(4): e791. https://doi.org/10.1093/forestscience/48.4.791

Espada M, Silva AC, van den Akker SE, Peter JA, Cock, Mota M, Jones JT (2016) Identification and characterization of parasitism genes from the pinewood nematode *Bursaphelenchus xylophilus* reveals a multilayered detoxification strategy. Molecular Plant Pathology 17(2): 286–295. https://doi.org/10.1111/mpp.12280

Foit J, Čermák V, Gaar V, Hradil K, Nový V, Rolincová P (2019) New insights into the life history of *Monochamus galloprovincialis* can enhance surveillance strategies for the pinewood nematode. Journal of Pest Science 92(3): 1203–1215. https://doi.org/10.1007/s10340-019-01110-y

Glass NL, Donaldson GC (1995) Development of primer sets designed for use with the PCR to amplify conserved genes from filamentous ascomycetes. Applied and Environmental Microbiology 61(4): 1323–1330. https://doi.org/10.1128/aem.61.4.1323-1330.1995

Gorton C, Webber JF (2000) Reevaluation of the status of the bluestain fungus and bark beetle associate *Ophiostoma minus*. Mycologia 92(6): 1071–1079. https://doi.org/10.1080/00275514.2000.12061254

Hall TA (1999) BIOEDIT: A user-friendly biological sequence alignment editor and analysis program for Windows 95/98/NT. Nucleic Acids Symposium Series 41: 95–98.

Hyde KD, Norphanphoun C, Maharachchikumbura SSN, Bhat DJ, Jones EBG, Bundhun D (2020) Refined families of Sordariomycetes. Mycosphere : Journal of Fungal Biology 11(1): 305–1059. https://doi.org/10.5943/mycosphere/11/1/7

Jacobs K, Bergdahl DR, Wingfield MJ, Halik S, Seifert KA, Bright DE, Wingfield BD (2004) *Leptographium wingfieldii* introduced into North America and found associated with exotic *Tomicus piniperda* and native bark beetles. Mycological Research 108(4): 411–418. https://doi.org/10.1017/S0953756204009748

Jankowiak R (2008) Fungi associated with *Tomicus minor* on *Pinus sylvestris* in Poland and their succession into the sapwood of beetle-infested windblown trees. Canadian Journal of Forest Research 38(10): 2579–2588. https://doi.org/10.1139/X08-101

Jankowiak R, Solheim H, Bilański P, Marincowitz S, Wingfield MJ (2020) Seven new species of *Graphilbum* from conifers in Norway, Poland and Russia. Mycologia 112(6): 1240–1262. https://doi.org/10.1080/00275514.2020.1778375

Ji YC, Zhang QM, Zhou CG, Liu ZY (2021) Risk Analysis of Pine Wilt Disease in Shandong Province. Journal of Shandong Agricultural University 52(02): 219–223. [Natural Science]

Jung J, Han H, Ryu SH, Kim W (2010) Microsatellite variation in the pinewood nematode, *Bursaphelenchus xylophilus* (Steiner and Buhrer) Nickle in South Korea. Genes & Genomics 32(2): 151–158. https://doi.org/10.1007/s13258-009-0842-7

Katoh K, Standley DM (2013) MAFFT multiple sequence alignment software version 7: Improvements in performance and usability. Molecular Biology and Evolution 30(4): 772–780. https://doi.org/10.1093/molbev/mst010

Kikuchi T, Cotton JA, Dalzell JJ, Hasegawa K, Kanzaki N, McVeigh P, Takanashi T, Tsai IJ, Assefa SA, Cock PJA, Otto TD, Hunt M, Reid AJ, Sanchez-Flores A, Tsuchihara K, Yokoi T, Larsson MC, Miwa J, Maule AG, Sahashi N, Jones JT, Berriman M (2011) Genomic Insights into the Origin of Parasitism in the Emerging Plant Pathogen *Bursaphelenchus xylophilus*. PLoS Pathogens 7(9): e1002219. https://doi.org/10.1371/journal.ppat.1002219

Kobayashi T, Sasaki K, Mamiya Y (1974) Fungi Associated with *Bursaphelenchus lignicolus*, the Pine Wood Nematode. Nihon Shinrin Gakkaishi 56(4): 136–145. https://doi.org/10.11519/jjfs1953.56.4_136

Kobayashi F, Yamane A, Ikeda T (1984) The Japanese pine sawyer beetle as the vector of pine wilts disease. Annual Review of Entomology 29(1): 115–135. https://doi.org/10.1146/annurev.en.29.010184.000555

Kumar S, Stecher G, Tamura K (2016) MEGA7: Molecular evolutionary genetics analysis version 7.0 for bigger datasets. Molecular Biology and Evolution 33(7): 1870–1874. https://doi.org/10.1093/molbev/msw054

Linit MJ, Kondo E, Smith MT (1983) Insects associated with the pinewood nematode, *Bursaphelenchus xylophilus* (Nematoda: Aphelenchoididae), in Missouri. Environmental Entomology 12(2): 457–470. https://doi.org/10.1093/ee/12.2.467

Liou J, Shih J, Tzean S (1999) *Esteya*, a new nematophagous genus from Taiwan, attacking the pinewood nematode (*Bursaphelenchus xylophilus*). Mycological Research 103(2): 242–248. https://doi.org/10.1017/S0953756298006984

Luchi N, Oliveira Longa CM, Danti R, Capretti R, Maresi G (2014) *Diplodia sapinea*: The main fungal species involved in the colonization of pine shoots in Italy. Forest Pathology 44(5): 372–381. https://doi.org/10.1111/efp.12109

Lun YY, Wang HM, Lu Q, Liu HX, Yao XH, Jiang WZ, Zhang XY (2019) Dominantly Ophiostomatoid fungus inhabiting tunnels and pupal chambers of *Monochamus alternatus* in pines infected by *Bursaphelenchus xylophilus*. Journal of Beijing Forestry University 41(06): 102–110.

Mota MM, Vieira PC (2008) Pine wilt disease: a worldwide threat to forest ecosystems. Springer, Dordrecht, 1–10. http://www.springerlink.com/index/10.1007/978-1-4020-8455-3

Pimentel CS, Firmino PN, Ayres MP (2021) Interactions between pinewood nematodes and the fungal community of pine trees. Fungal Ecology 51: e101046. https://doi.org/10.1016/j.funeco.2021.101046

Rambaut A, Drummond AJ, Xie D, Baele G, Suchard MA (2018) Posterior summarization in Bayesian phylogenetics using Tracer 1.7. Systematic Biology 67(5): 901–904. https://doi.org/10.1093/sysbio/syy032

Rayner RW (1970) A mycological colour chart. Commonwealth Mycological Institute and British Mycological Society.

Robertson L, Arcos SC, Escuer M, Santiago MR, Esparrago G, Abelleira A, Navas A (2011) Incidence of the pinewood nematode *Bursaphelenchus xylophlius* Steiner & Buhrer, 1934 (Nickle, 1970) in Spain. Nematology 13(6): 755–757. https://doi.org/10.1163/138855411X578888

Ronquist F, Teslenko M, van der Mark P, Ayres DL, Darling A, Höhna S, Larget B, Liu L, Suchard MA, Huelsenbeck JP (2012) MrBayes 3.2: Efficient Bayesian phylogenetic inference and model choice across a large model space. Systematic Biology 61(3): 539–542. https://doi.org/10.1093/sysbio/sys029

Rumbold CT (1936) Three blue-staining fungi, including two new species, associated with bark beetles. US Government Printing Office.

Ryss A, Vieira P, Mota M, Kulinich O (2005) A synopsis of the genus *Bursaphelenchus Fuchs*, 1937 (Aphelenchida: Parasitaphelenchidae) with keys to species. Nematology 7(3): 393–458. https://doi.org/10.1163/156854105774355581

Sartaj AS, Kazunori S, Kazuyuki I (2011) Effect of *Penicillium* sp. EU0013 inoculation on tomato growth and *Fusarium* wilt. Horticulture Research 65: 69–73.

Seifert KA, Webber JF, Wingfield MJ (1993) Methods for studying species of *Ophiostoma* and *Ceratocystis*. In: Wingfield MJ, Seifert KA, Webber JF (Eds) *Ceratocystis* and *Ophiostoma*: taxonomy, ecology and pathogenicity. The American Phytopathological Society Press, Minnesota, USA, 255–259.

Solheim H (1992a) Fungal succession in the sapwood of Norway spruce infested by the bark beetle *Ips typographus*. European Journal of Forest Pathology 22(3): 136–148. https://doi.org/10.1111/j.1439-0329.1992.tb01440.x

Solheim H (1992b) The early stages of fungal invasion in Norway spruce infested by the bark beetle *Ips typographus*. Canadian Journal of Botany 70(1): 1–5. https://doi.org/10.1139/b92-001

Sriwati R, Takemoto S, Futai K (2007) Cohabitation of the pine wood nematode, *Bursaphelenchus xylophilus*, and fungal species in pine trees inoculated with *B. xylophilus*. Nematology 9(1): 77–86. https://doi.org/10.1163/156854107779969655

Stamatakis A (2014) RaxML version 8: A tool phylogenetic analysis and postanalysis of large phylogenies. Bioinformatics (Oxford, England) 30(9): 1312–1313. https://doi.org/10.1093/bioinformatics/btu033

State Forestry Administration of the People's Republic of China (2021) Announcement of State Forestry Administration of the People's Republic of China No. 5. https://www.forestry.gov.cn/main/3457/20210329/151957233445926.html

Swofford DL (2003) PAUP*: phylogenetic analysis using parsimony, version 4.0 b10.

Togashi K, Jikumaru S (2007) Evolutionary change in a pine wilt system following the invasion of Japan by the pinewood nematode, *Bursaphelenchus xylophilus*. Ecological Research 22(6): 862–868. https://doi.org/10.1007/s11284-007-0339-2

Upadhyay HP (1981) A monograph of *Ceratocystis* and *Ceratocystiopsis.* University of Georgia Press, Athens 36(2): 175. https://doi.org/10.1007/BF02858713

Villarreal M, Ruelo V, De Tov AMT, Arenal E (2005) A new *Ophiostoma* species isolated from. Mycotaxon 92: 259–268.

Wang CY, Fang ZM, Wang Z, Zhang DL, Gu LJ, Lee MR, Liu L, Sung CK (2011) Biological control of the pinewood nematode *Bursaphelenchus xylophilus* by application of the endoparasitic fungus *Esteya vermicola*. BioControl 56(1): 91–100. https://doi.org/10.1007/s10526-010-9302-1

Wang HM, Lun YY, Lu Q, Liu HX, Decock C, Zhang XY (2018) Ophiostomatoid fungi associated with pines infected by *Bursaphelenchus xylophilus* and *Monochamus alternatus* in China, including three new species. MycoKeys 1(39): 1–27. https://doi.org/10.3897/mycokeys.39.27014

Wang HM, Wang Z, Liu F, Wu CX, Zhang SF, Kong XB, Decock C, Lu Q, Zhang Z (2019) Differential patterns of ophiostomatoid fungal communities associated with three sympatric *Tomicus* species infesting pines in south-western China, with a description of four new species. MycoKeys 50: 93–133. https://doi.org/10.3897/mycokeys.50.32653

Wang Z, Liu Y, Wang HM, Meng XJ, Liu XW, Decock C, Zhang XY, Lu Q (2020) Ophiostomatoid fungi associated with *Ips subelongatus*, including eight new species from northeastern China. IMA Fungus 11(1): e3. https://doi.org/10.1186/s43008-019-0025-3

White TJ, Bruns T, Lee SJWT, Taylor JL (1990) Amplification and direct sequencing of fungal ribosomal RNA genes for phylogenetics. PCR protocols: a guide to methods and applications 18(1): 315–322. https://doi.org/10.1016/B978-0-12-372180-8.50042-1

Wijayawardene NN, Hyde KD, Dai DQ, Sánchez-García M, Goto BT, Saxena RK, Erdoğdu M, Selçuk F, Rajeshkumar KC, Aptroot A, Błaszkowski J, Boonyuen N, da Silva GA, de Souza FA, Dong W, Ertz D, Haelewaters D, Jones EBG, Karunarathna SC, Kirk PM, Kukwa M, Kumla J, Leontyev DV, Lumbsch HT, Maharachchikumbura SSN, Marguno F, Martínez-Rodríguez P, Mešić A, Monteiro JS, Oehl F, Pawłowska J, Pem D, Pfliegler

WP, Phillips AJL, Pošta A, He MQ, Li JX, Raza M, Sruthi OP, Suetrong S, Suwannarach N, Tedersoo L, Thiyagaraja V, Tibpromma S, Tkalčec Z, Tokarev YS, Wanasinghe DN, Wijesundara DSA, Wimalaseana SDMK, Madrid H, Zhang GQ, Gao Y, Sánchez-Castro I, Tang LZ, Stadler M, Yurkov A, Thines M (2022) Outline of Fungi and fungus-like taxa – 2021. Mycosphere: Journal of Fungal Biology 13(1): 53–453. https://doi.org/10.5943/mycosphere/13/1/2

Win TT, Bo B, Malec P, Fu P (2021) The effect of a consortium of *Penicillium* sp. and *Bacillus* spp. in suppressing banana fungal diseases caused by *Fusarium* sp. and *Alternaria* sp. Journal of Applied Microbiology 131(4): 1890–1908. https://doi.org/10.1111/jam.15067

Ye JR (2019) Epidemic status of pine wilt disease in China and its prevention and control techniques and counter measures. Linye Kexue 55(9): 1–10.

Zeng FY, Luo YQ, Lu Q, Liang J, Zhang XY (2006) Studies on the mycoflora of *Pinus thunbergii* infected by *Bursaphelenchus xylophilus*. Forest Research 19(4): 537–540.

Zhang W, Wang X, Li YX, Liu ZK, Li DZ, Wen XJ, Feng YQ, Zhang XY (2021) Pinewood Nematode Alters the Endophytic and Rhizospheric Microbial Communities of *Pinus massoniana*. Microbial Ecology 81(3): 807–817. https://doi.org/10.1007/s00248-020-01619-1

Zhao LL, Sun JH (2017) Pinewood Nematode *Bursaphelenchus xylophilus* (Steiner and Buhrer) Nickle. In: Wan F, Jiang M, Zhan A (Eds) Biological Invasions and Its Management in China. Invading Nature - Springer Series in Invasion Ecology vol 13. Springer, Singapore. https://doi.org/10.1007/978-981-10-3427-5_1

Zhao LL, Lu M, Niu H, Zhang S, Sun J (2013) A native fungal symbiont facilitates the prevalence and development of an invasive pathogen-native vector symbiosis. Ecology 94(12): 2817–2826. https://doi.org/10.1890/12-2229.1

Zhao LL, Mota M, Vieira P, Butcher RA, Sun J (2014) Interspecific communication between pinewood nematode, its insect vector, and associated microbes. Trends in Parasitology 30: 299–308. https://doi.org/10.1016/j.pt.2014.04.007

Zhao LL, Ahmad F, Lu M, Zhang W, Wickham JD, Sun J (2018) Ascarosides Promote the Prevalence of Ophiostomatoid Fungi and an Invasive Pathogenic Nematode, *Bursaphelenchus xylophilus.* Journal of Chemical Ecology 44(7–8): 701–710. https://doi.org/10.1007/s10886-018-0996-3

Zheng YN, Liu PX, Shi Y, Wu H, Yu HY, Jiang SW (2021) Difference analysis on pine wilt disease between Liaoning Province of northeastern China and other epidemic areas in China. Journal of Beijing Forestry University 43(5): 155–160. https://doi.org/10.12171/j.1000-1522.20200108

Zhou X, Burgess TI, De Beer ZW, Lieutier F, Yart A, Klepzig K, Wingfield MJ (2007) High intercontinental migration rates and population admixture in the sapstain fungus *Ophiostoma ips.* Molecular Ecology 16(1): 89–99. https://doi.org/10.1111/j.1365-294X.2006.03127.x

Zhu YQ, Huang WY, Xie WL, Ma Y, Wen XJ, Wang J (2021) Research progress on control methods of pine wilt disease. Hebei Forestry Science and Technology (02): 44–48. https://doi.org/10.16449/j.cnki.issn1002-3356.2021.02.010